

One-dimensional van der Waals heterostructures

Rong Xiang^{1,12*}, Taiki Inoue^{1,12}, Yongjia Zheng^{1,12}, Akihito Kumamoto², Yang Qian¹, Yuta Sato³, Ming Liu¹, Devashish Gokhale⁴, Jia Guo^{1,5}, Kaoru Hisama¹, Satoshi Yotsumoto¹, Tatsuro Ogamoto¹, Hayato Arai¹, Yu Kobayashi⁶, Hao Zhang¹, Bo Hou⁷, Anton Anissimov⁸, Yasumitsu Miyata^{6,9}, Susumu Okada¹⁰, Shohei Chiashi¹, Yan Li^{1,5}, Esko I. Kauppinen¹¹, Yuichi Ikuhara², Kazu Suenaga³, Shigeo Maruyama^{1,7,*}

¹ *Departure of Mechanical Engineering, The University of Tokyo, Tokyo 113-8656, Japan*

² *Institute of Engineering Innovation, The University of Tokyo, Tokyo, Japan*

³ *National Institute of Advanced Industrial Science and Technology (AIST), AIST Central 5, Tsukuba 305-8565, Japan*

⁴ *Department of Chemical Engineering, Indian Institute of Technology Madras, Chennai 600036, India*

⁵ *College of Chemistry and Molecular Engineering, Peking University, Beijing 100871, China*

⁶ *Department of Physics, Tokyo Metropolitan University, Hachioji, Tokyo 192-0397, Japan*

⁷ *Energy Nano Engineering Lab., National Institute of Advanced Industrial Science and Technology (AIST), Ibaraki 305-8564, Japan*

⁸ *Canatu Ltd., Konalankuja 5, FI - 00390 Helsinki, Finland.*

⁹ *JST-PRESTO, Kawaguchi, Saitama 332-0012, Japan*

¹⁰ *Graduate School of Pure and Applied Sciences, University of Tsukuba, Tsukuba, Ibaraki 305-8571, Japan*

¹¹ *Department of Applied Physics, Aalto University School of Science, 15100, FI-00076 Aalto, Finland*

¹² *These authors contributed equally. Rong Xiang, Taiki Inoue, Yongjia Zheng*

*email: xiangrong@photon.t.u-tokyo.ac.jp; maruyama@photon.t.u-tokyo.ac.jp

Property by design is one appealing idea in material synthesis but hard to achieve in practice. A recent successful example is the demonstration of van der Waals (vdW) heterostructures,¹⁻³ in which atomic layers are stacked on each other and different ingredients can be combined with a large freedom. This concept, usually described as a nanoscale Lego blocks, allows to build sophisticated structures layer by layer. However, this concept has been so far limited in two dimensional (2D) materials. Here we show a class of new material where different layers are co-axially (instead of planarly) stacked. As the structure is in one dimensional (1D) form, we name it “1D vdW heterostructures”. We demonstrate a 5 nm diameter nanotube consisting 3 different materials: an inner conductive carbon nanotube (CNT), a middle insulating hexagonal boron nitride nanotube (BNNT) and an outside semiconducting MoS₂ nanotube. As the technique is highly possible to be applicable to most of other materials in the current 2D libraries [Liu Zheng et al., Nature 2018], we anticipate our strategy to be a starting point for discovering a class of new semiconducting nanotube materials. Also a plethora of sophisticated 1D heterostructures may appear after the combination of CNTs and BNNTs.

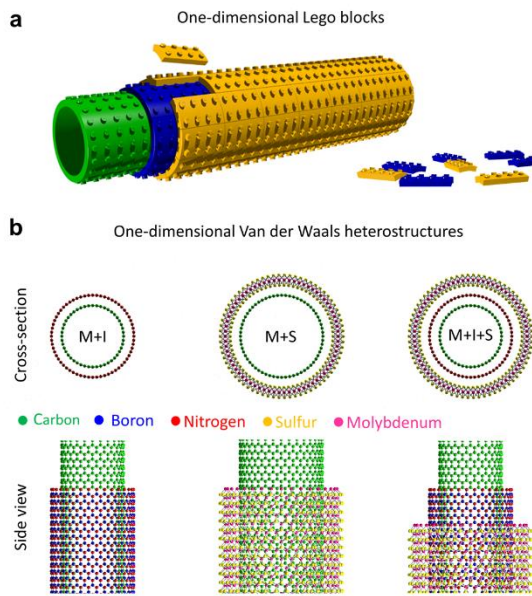


Figure 1 Overview of the current study. (a) A one dimensional Lego block showing the concept of this work: atomic layers of different materials can be co-axially stacked to form a 1D vdW heterostructure; (b) the atomic model of the materials built in this study: 1D metal-insulator (M+I) heterostructure of SWCNT and BNNT, 1D metal-semiconducting (M+S) heterostructures of SWCNT-MoS₂, and ternary 1D metal-insulator-semiconducting (M+I+S) heterostructure.

When playing Lego blocks, one usually starts from a green baseplate, on which various structures are built. In this study, the baseplate is single-walled carbon nanotube (SWCNT). SWCNT is chosen as this starting material for several reasons. First and foremost it is so far the best-studied 1D material and can be synthesized in many controlled geometries. Second, SWCNT can be a good conductor so it may serve as the

electrode for a future device. The SWCNT film (which we used in most of the following demonstrations) has a sheet resistance about 80 ohm/sq. at 90%, comparable to the Indium Tin Oxide (ITO) films that are widely used in modern technology.⁴

The first example we demonstrate is SWCNT-BN 1D heterostructures. Figure 2a shows a representative TEM image of this coaxially wrapped material and more images are provided as Figure S1. From a conventional TEM image, this nanotube looks not distinguishable from a triple-walled pure carbon nanotube. The cs-corrected image of a similar tube reveal a contrast of stacking of two perfect nanotubes. However, as the starting material is purely single-walled before we performed a post BN coating, it is reasonable to expect that the outer wall(s) are h-BN. This point is evidenced by electron energy loss spectroscopy (EELS) shown Figure 2d. Another EELS mapping is shown as Figure S2. Also as the reactions occurs on the outer surface, different from previous attempts inside a nanotube,^{5,6} continuous coating up to micrometer can be achieved in this work.

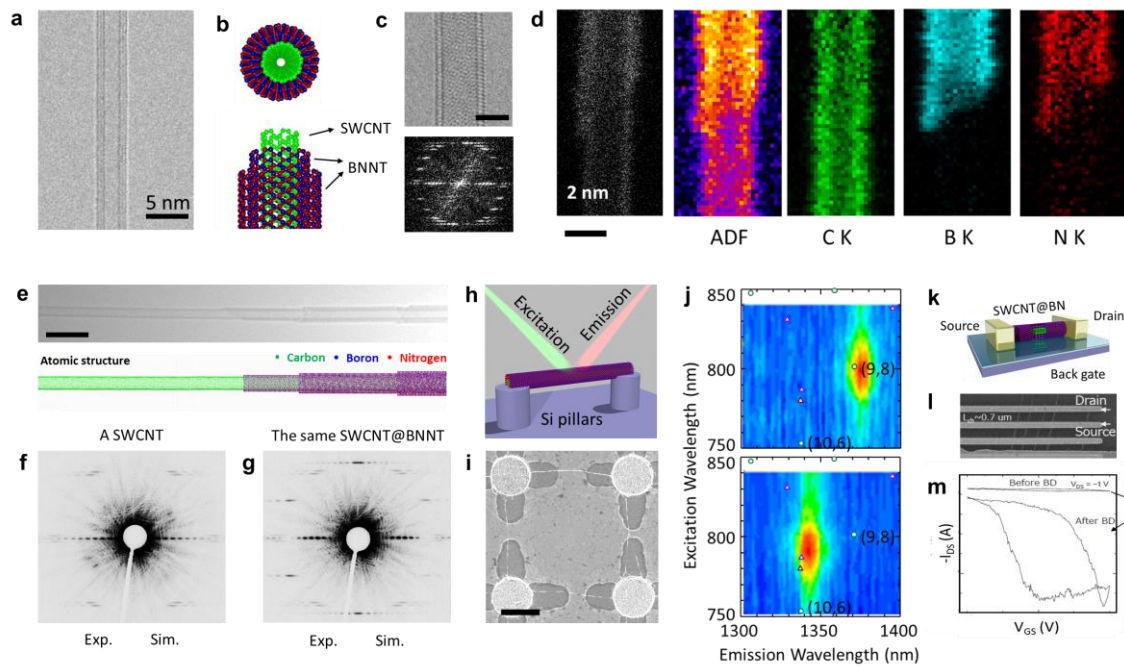


Figure 2 SWCNT-BN coaxial nanotubes. (a) TEM image and (b) atomic models of a SWCNT wrapped with two layer of BNNT; (c) cs-TEM image of a SWCNT-BN nanotube and (c) its FFT; (d) EELS mapping of a SWCNT partially wrapped with BN nanotube showing the inner is carbon and outer is BN; (e) TEM images of SWCNT-BN steps and its atomic model; (f) ED pattern of a (16,14) SWCNT and (f) the ED pattern of the same nanotube after wrapping with a (34, 0) BNNT; (h) a schematic and SEM image of SWCNT-BN nanotube grown bridging the pillars; (j) PL excitation-emission map of as suspended (9,8) SWCNT with and without BN coating; (k) a schematic, (l) SEM and (m) characteristic transfer curve of a FET built on a SWCNT-BN arrays.

This co-axial structure can be characterized by many other techniques. XPS

reveals B-N bond and C-C bond in this sample but no C-N and B-C, suggesting there is no noticeable substitution of atoms (Figure S3); Raman spectra of the SWCNT-BN (Figure S4) show clear features for the inner SWCNTs, evidencing the high quality of is preserved (this will be further supported later); Cathode luminance spectra (Figure S5) of the sample confirms the existence of outer BN by emissions at UV range; optical absorption spectra (Figure S6) reveals an emerge of peak near 200-300 nm. When extending growth time, the number of outside BN layers increase. (Figure S7) Dominantly 1-2 layer to 5-8 layers can be tuned. Also, the growth strategy applies to SWCNTs with different morphologies. We confirmed BN can be successfully coated onto various SWCNTs including vertically arrays, random networks and suspended SWCNTs bridging pillars. (Figure S8)

The formation of this SWCNT-BN structure follows an open-end growth mechanism. (Movie S1) As the outside BN is post-grown, the extension of BNNT happens only at the open edge of BNNT. This is similar to the growth of an additional layer in 2D material, but very rarely observed in previous growth of carbon nanotubes.⁷ This open edge growth mechanism is evidenced by the many growth steps observed in an intermediated growth condition (Figure 2e). These steps also allow to take electron diffraction of the pristine SWCNT and the same tube after BN wrapping. In Figure 2f and

g, a (16,14) SWCNT is wrapped by a (34, 0) SWBNNT. (Another example shown in Figure S9) Even without the steps, the 2% of lattice difference between SWCNT and BNNT allows to identify them in the ED patterns. We performed chiral angle analysis shown (Figure S10, Table S1). In a collection of 74 SWCNTs and 40 SWCNT-BNNT double walled nanotubes, SWCNTs are enriched in near arm-chaired side. This armchair enrichment is consistent with previous experimental and theoretical analysis.⁸ However, the outer BNNTs are evenly distributed (even slightly prefers zigzag side). This distinct difference may be attributed the open-end growth model, which is different from the catalytic growth of pristine SWCNT. Nonetheless, it is clearly no strict chiral angle dependence in this SWCNT-BN heterostructures. This is also consistent with the concept of vdW heterostructures that lattice matching is not a requirement for material combination. It is also a critical point for the incorporation other material that have larger lattice mismatch.

BN coating does not change the intrinsic transport property of inner SWCNT. A field effect transistor building on this BN wrapped SWCNT show a similarly high performances with the ON/OFF ratio of 10^6 and a mobility of xxx. (Figure S11) However, it significantly changes the physical and chemical properties of the tube as the surface-related is protected/isolated from the surrounding environment. One first example is that

thermal stability in air. Pure SWCNTs are well known to burn in air at a temperature around 450°C. After coating, the structure survives at up to 700°C. (Figure S12) A second example is photoluminescence (PL). When a semi-conducting SWCNT is excited by a photon with high energy, it emits a photon with the energy close to its optical band-gap. This energy however can be easily shifted by the surface condition of the SWCNT.⁹ We found the PL of pristine SWCNT usually located at (called “air state”) but the BN coated can be routinely observed emitting PL at a blue-shifted position (called “vacuum state”). We interpret this as the protection effect of outside BN, which means the SWCNT is isolated from the molecules in air by a single- or few-layer BN wrapping. (A more detailed comparison shown as Figure S13)

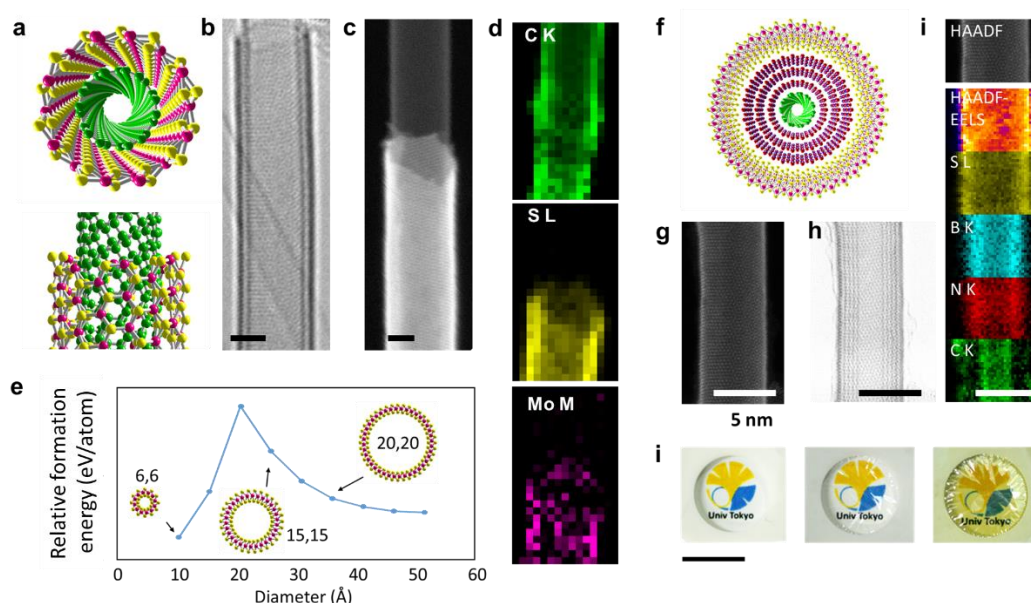


Figure 3 SWCNT-MoS₂ 1D heterostructure and SWCNT-BNNT-MoS₂ 1D

heterostructure. (a) Atomic model, (b) TEM image and (c) STEM-HAADF image of a single-walled MoS₂ nanotube grown on a SWCNT; (b) the relative formation energy of a single-walled MoS₂ nanotube as a function of tube diameter calculated by molecule dynamics simulation; (e) atomic model, (f) STEM-HAADF image (g) TEM image and (h) EELS mapping of a 5 nm diameter ternary 1D wdW heterostructures consisting one layer of carbon, three layers of BN and one layer MoS₂ nanotube; (i) optical images of pristine SWCNT and coated nanotubes.

The successful post-stacking of BNNT onto the outer surface of SWCNTs makes us believe a similar strategy may be employed to build other more sophisticated structures, or even those materials ever-existed. Single-walled MoS₂ nanotube is one example. MoS₂ 2D sheet is intensively studied as the representative of transition metal dichalcogenide (TMD) material. Single-walled MoS₂ nanotube is, however, not convincingly demonstrated in previous experiments. Figure 3a-c show the atomic structure and TEM images of SWCNT-MoS₂ coaxial nanotube obtained after applying the strategy. The MoS₂ nanotube distinguishes itself by a much stronger contrast than carbon in both TEM and STEM images. (More images are shown Figure S14) This is as far as we know one of the first TEM images evidencing the existence of single-walled

MoS₂ nanotube. We emphasize there single-walled MoS₂ nanotube because multi-walled tubes (usually 20 nm or above) are observed before. Also, single-walled MoS₂ nanotube is predicted to have direct band-gap so its properties can probably be distinctively different from its thicker multi-walled counterparts.¹⁰ Also, quantum confinement is expected to be significant in a single-walled MoS₂ nanotube with this small diameter.[ref needed] Most importantly, formation of a MoS₂ nanotube suggests that other TMD nanotubes may also be produced by a similar approach. If so, we foresee a lot interesting research topics spectroscopy, device, and others, for this single-layer feature, largely curved, quantum-confineable TMD nanotubes.

However, we notice is this MoS₂ nanotube is much more difficult to synthesize than BNNTs. The yield of MoS₂ nanotube is very low and most SWCNTs are not coated. Possible reasons are speculated to be: 1) larger mismatch of MoS₂ tube and SWCNT (BN: 2% vs. MoS₂: 25%); or 2) larger curvature energy due to thickness (MoS₂ has 3 atomic layers). Since we clearly learned from the previous SWCNT-BN system that there is no strong relationship between inner and outer walls, the thickness effect could be more likely. To understand this point, we performed a molecular dynamics simulation on the formation energy of single-walled MoS₂ nanotubes with different diameter. A clear $1/D^2$ relationship is observed in Figure 3d, which suggests that, in small diameter range,

formation energy is significantly higher than tubes larger than 3.5 nm. This result is comparable to a previous density function theory (DFT) calculation.¹¹ In that work, the stable MoS₂ nanotubes are predicted to be above 3.5 nm. This prediction is surprisingly consistent with our experiment observations. The tubes shown in (Figure S14) have diameter ranging from 3.5 – 4.5 nm. In addition, there is no clear evidence showing preference of zigzag or armchair MoS₂ nanotube but we speculate their growth should be kinetically different. Besides this, many features of this single-walled MoS₂ nanotube is unknown, and we expect more efforts to come for this new material.

Finally we demonstrate a ternary, SWCNT-BN-MoS₂ coaxial nanotube, shown in Figure 3e-g. It is 5 nm in diameter but contains three different materials: an inner one layer of conducting carbon, a middle three layers of insulating hexagonal boron nitride and an outside one layer of semiconducting MoS₂. This structure is clearly visualized by the EELS mapping in Figure 3h. Also, as the tube diameter SWCNT increase from 2 to more than 3 nm after BN coating, synthesizing an additional of MoS₂ nanotube becomes much easier. More efficient growth are observed on most of the isolated regions. The coating can be produced in centimeter scale, and clearly difference can be observed for original SWCNT, SWCNT-BN, SWCNT-BN-MoS₂ film even with naked eyes (Figure 3i). The optical absorption spectrum of the sample clearly reveals the photon absorption

from three different layers.

In conclusion, we extended the concept of van der waals heterostructures to a different dimension. It is highly possible that the synthetic technique shown here can be employed to generate a class of new nanotube materials, and a series of more sophisticated heterostructures.

Reference

- 1 Geim, A. K. & Grigorieva, I. V. Van der Waals heterostructures. *Nature* **499**, 419-425, doi:10.1038/nature12385 (2013).
- 2 Novoselov, K. S., Mishchenko, A., Carvalho, A. & Neto, A. H. C. 2D materials and van der Waals heterostructures. *Science* **353**, doi:ARTN aac9439 10.1126/science.aac9439 (2016).
- 3 Liu, Y. *et al.* Van der Waals heterostructures and devices. *Nat Rev Mater* **1**, doi:UNSP 16042 10.1038/natrevmats.2016.42 (2016).
- 4 Nasibulin, A. G. *et al.* Multifunctional Free-Standing Single-Walled Carbon Nanotube Films. *Acs Nano* **5**, 3214-3221, doi:10.1021/nn200338r (2011).
- 5 Nakanishi, R. *et al.* Thin single-wall BN-nanotubes formed inside carbon nanotubes. *Sci Rep-Uk* **3**, doi:ARTN 1385 10.1038/srep01385 (2013).
- 6 Arenal, R. & Lopez-Bezanilla, A. In Situ Formation of Carbon Nanotubes Encapsulated within Boron Nitride Nanotubes via Electron Irradiation. *Acs Nano* **8**, 8419-8425, doi:10.1021/nn502912w (2014).
- 7 Yao, Y. G., Feng, C. Q., Zhang, J. & Liu, Z. F. "Cloning" of Single-Walled Carbon Nanotubes via Open-End Growth Mechanism. *Nano Lett* **9**, 1673-1677, doi:10.1021/nl900207v (2009).
- 8 Ding, F., Harutyunyan, A. R. & Yakobson, B. I. Dislocation theory of chirality-controlled nanotube growth. *P Natl Acad Sci USA* **106**, 2506-2509, doi:10.1073/pnas.0811946106 (2009).
- 9 Chiashi, S., Watanabe, S., Hanashima, T. & Homma, Y. Influence of Gas Adsorption on Optical Transition Energies of Single-Walled Carbon Nanotubes. *Nano Lett* **8**, 3097-3101, doi:10.1021/nl801074j (2008).
- 10 Seifert, G., Terrones, H., Terrones, M., Jungnickel, G. & Frauenheim, T. Structure and electronic properties of MoS₂ nanotubes. *Phys Rev Lett* **85**, 146-149, doi:DOI 10.1103/PhysRevLett.85.146 (2000).
- 11 Zhang, D. B., Dumitrica, T. & Seifert, G. Helical Nanotube Structures of MoS₂ with Intrinsic Twisting: An Objective Molecular Dynamics Study. *Phys Rev Lett* **104**, doi:ARTN 065502 10.1103/PhysRevLett.104.065502 (2010).